Sci. Annals, Fac. Phys. & Mathem., Univ. Thessaloniki, **16**, 423 (1976)

COMPUTED INTENSITY PROFILES OF DISLOCATION RIBBONS

by

P. GRIGORIADIS

(Physics Department, University of Thessaloniki)

(Introduced by Prof. N. Economou)

(Received 20.12.76)

Abstract. *The observed width of a dislocation ribbon in electron microscopy is expected to be different from the true separation of its partial dislocations due to image shift of dislocations relative to their core positions. Calculations of intensity profiles of dislocation ribbons are performed in order to investigate the effect of this phenomenon on the stacking fault energy calculations using the ribbon width method:*

The results show that in the case of $SiTe_2$ the observed ribbon widths are about 1% greater than the true ones and this effect is well within the experimental errors to affect the estimated value of the stacking fault energy.

1. INTRODUCTION

Theoretical calculations of dislocation intensity profiles using the dynamical theory of electron diffracrion including absorption showed a shift of the dislocation peak intensity from the true dislocation core position[1]. This shift depends on the dislocation character i.e the angle (α) between its dislocation line direction and its Burgers vector as well as on its depth in the crystal and the imaging conditions. Moreover, a perfect dislocation lying in the main glide plane of a close-packed structure can dissociate into a ribbon of two parallel partial dislocations bounding a stacking fault according to the scheme

$$AB \longrightarrow A\sigma + \sigma B$$

where AB leads from one atom position to the next equivalent one in a close-packed plane, Fig. (1). Perfect dislocations have Burgers vectors AB, AC, BC; partials $A\sigma$, $B\sigma$, $C\sigma$:

It is seen from Fig. (1) that the Burgers vectors of partials make an angle of 60°. The shift of each partial relative to its core will be different in each case thus affecting the observed ribbon width.

In the present work this effect is investigated in order to decide for the error introduced in the calculated value of the stacking fault energy based on ribbon width measurements. The results can be applied to any cubic or hexagonal close packed structure. However, the experimental conditions are chosen to fit $SiTe_2$ crystal which is a hexagonal layered-structure.

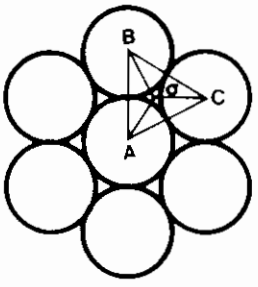

Fig. 1. Burgers vector notation.

2. TWO-BEAM DYNAMICAL EQUATIONS OF ELECTRON DIFFRACTION

For distorted crystals i.e crystals containing a defect such as a dislocation, the two-beam dynamical equations[2] of electron diffraction, based on the column approximation and including absorption, are a pair of complex first-order differential equations of the form:

$$dT/dZ = -NT + (i - A)\ S$$

$$dS/dZ = (i - A)T + [-N + 2iw + 2i \frac{d}{dZ} (\bar{g} \cdot \bar{R})]\ S \qquad (I)$$

Where T and S are the amplitudes of the electron waves in the directions of the indicent and diffracted beams. The parameters N and A are the normal and the anomalous absorption coefficients, while w is the deviation parameter from the exact Bragg reflecting conditions. The vectors $\bar{g}$ and $\bar{R}$ are the reflecting vector and the displacement vector of the defect respectively:

The real variable z in the vertical down direction parallel to electron beam has been changed to $Z = \frac{z}{\xi_g/\pi}$ for compntational purposes i.e the unit of lenght is $\frac{\xi_g}{\pi}$, where ξ_g is the two heam extinction distance.

The displacement vector $\bar{R}$ of a dislocation in isotropic crystals is given by

$$\bar{R} = \frac{1}{2\pi}\left\{\bar{b}\,\varphi + \bar{b}_e \frac{\sin 2\varphi}{4(1-\nu)} + \bar{b}\wedge\bar{u}\left[\frac{1-2\nu}{2(1-\nu)}\ln r + \frac{\cos 2\varphi}{4(1-\nu)}\right]\right\} \qquad (11)$$

where $\bar{b}$, $\bar{b}_e$ are the Burgers vector and its edge component respectively; the angle φ is indicated in Fig. (2) as φ_1 or φ_2; ν is the Poisson ratio and $\bar{u}$ is a unit vector in the positive sense of the dislocation.

3. PROGRAM GEOMETRY

The column approximation is illustrated in Fig. (2) for a crystal of thickness t. The two partial dislocations lying at depth y are perpendicular to the page at points O_1 and O_2 and parallel to the crystal surfaces:

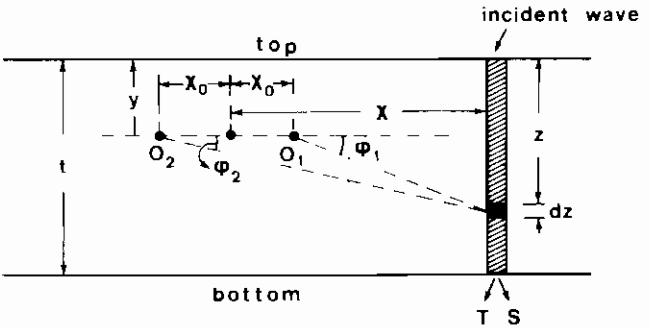

Fig. 2. The column approximation.

Both dislocations cause a displacement of an atom from its true position in the shaded slab of the column. The total resulting displacement is

$$\bar{R}_T = \bar{R}_1 + \bar{R}_2$$

The angles φ_1 and φ_2 can be expressed as functions of the coordinates x, y, z. The differential equations (I) are integrated numerically starting with T = 1 and S=O at Z=O (top surface of the crystal foil) down a column. The integration procedure uses the fourth-order Runge-Kutta method as modifiel by Merson[3] for estimating the truncation error of the integration and automatically choosing the optimum integration step size to satisfy a preassigned accuracy. At the exit sur-

face of the foil TT* and SS* give the intensity of a point in the bright field and dark field image profile respectively. The column is shifted to the right and the procedure is repeated.

4. EXPERIMENTAL CONDITIONS

The main glide plane coincides with the basal plane in crystals of h.c.p structure and it is also the cleavage plane in layered structures, like $SiTe_2$. A dislocation ribbon lying in the basal plane with its total Burgers vector b in this plane will satisfy the condition $\bar{g} . \bar{b} \wedge \bar{u} = 0$ when $\bar{g}$ is parallel to the foil plane i.e the crystal is untilted. This condition is satisfied in the present experiments and it reduces considerably the displacement vector eliminating the third term in the expression (II).

Moreover, the hexagonal crystals of layered structures are anisotropic and only the basal plane is isotropic[4]. This isotropicity allows one to take anisotropy into account for a dislocation lying in the basal plane and apply the results of the isotropic elasticity theory i.e to use equation (II), where the value of ν is given by $\nu = 1 - \frac{K_s}{K_e}$

and $K_s = (C_{44} C_{66})^{1/2}$

$$K_e = (\bar{C}_{11} + C_{13}) \left[\frac{C_{44} (C_{11} - C_{13})}{C_{33} (\bar{C}_{11} + C_{13} + 2C_{44})} \right]^{1/2}$$

$$\bar{C}_{11} = (C_{11} C_{33})^{1/2}$$

The C_{ij} are the elastic constants of the material. Unfortunately, these elastic constants are unknown for $SiTe_2$ and an effective value of $\nu = 0.43$ was determined[5] using the procedure of Amelinckx[6].

The Poisson ratio takes the value of $\nu = \frac{1}{3}$ in isotropic crystals.

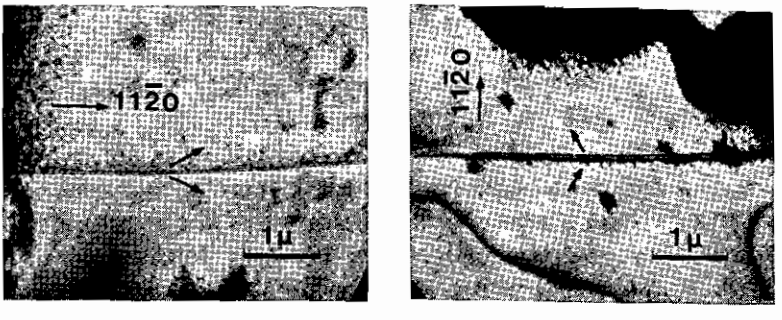

Fig. 3a, b. Experimental micrographs of different segments of a dislocation ribbon. Note the different widths in a) $a = 0^0$; in b) $a = 90^0$.

Fig. (3a,b) shows different segments of the same dislocation ribbon with both partials visible in $SiTe_2$. The reflecting vector and the Burgers vectors of the partials are also indicated: In Fig (3b) the total Burgers vector of the ribbon and its line direction enclose an angle of $\alpha=90^0$, while in Fig. (3α) $\alpha = 0^0$.

The calculated extinction distance of the operating reflection in Fig. (3a,b) is $\xi_g = 110$ Å and the deviation parameter is $w = 0.3$.

5. RESULTS AND DISCUSSION

The intensity distribution of the experimental micrographs in Fig. (3) is seen in Fig. (4): These curves are obtained from a microdensitometer.

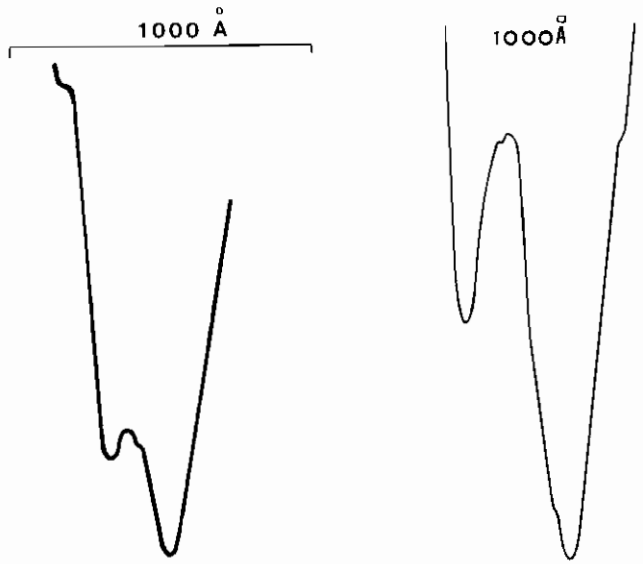

Fig. 4a, b. Microdensitometer traces corresponding to the experimental micrographs.

The calculated intensity profiles are shown in Fig. (5). The position of the partial dislocation cores are marked D. It is concluded that the ribbon width as determined by the calculated peak intesities is greater than the true width given by the core positions about 1% in all cases:

Thus, the non-coincidence of the true and the observed width is well within the experimental errors and will not affect the measured stacking fault energy of $SiTe_2$ by the ribbon width method.

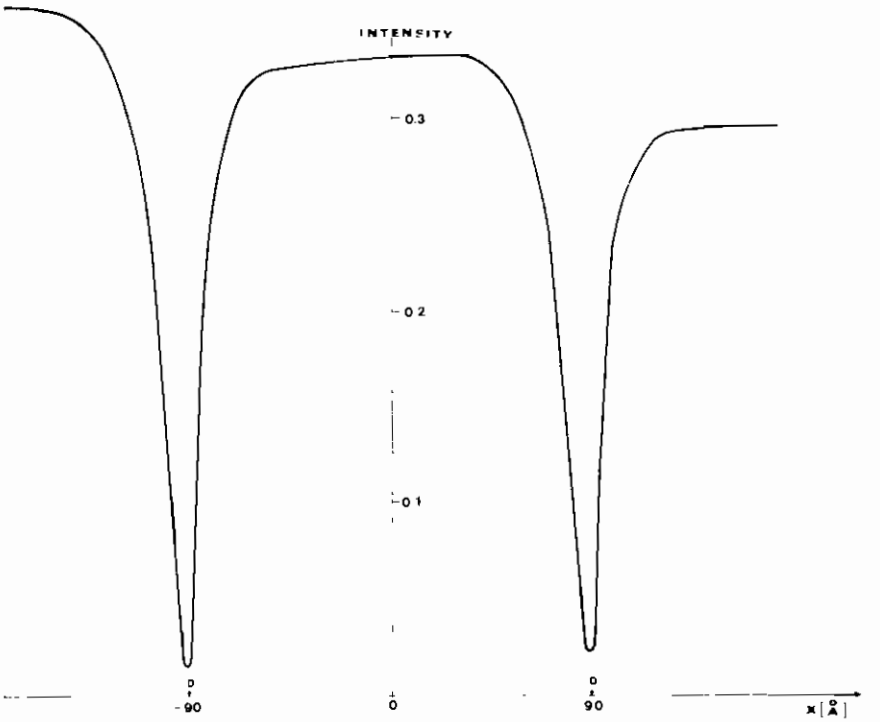

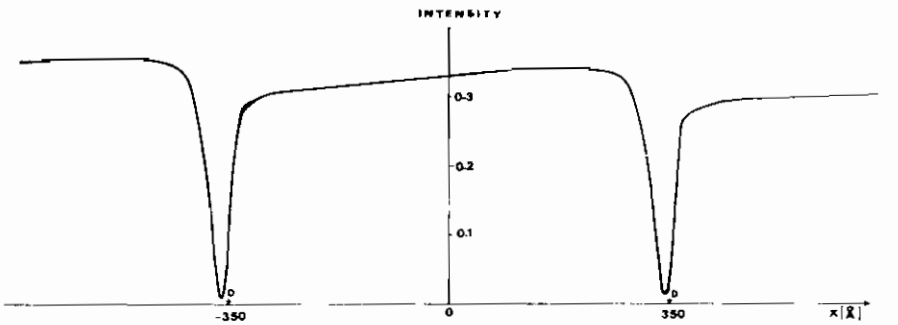

Fig. 5a, b. Computed bright-field intensity profiles corresponding to the experimental micrographs; $t = 8\xi_g$, $w = 0.3$ and $y = 4\xi_g$.

ACKNOWLEDGMENTS

The author is greatly indebted to Professors N. A. Economou and J. Stoemenos for suggesting the problem and for valuable discussions.

REFERENCES

1. P. E. Hirsch, A. Howie, R. B. Nicholson, D. W. Pashley and M. J. Whelan: Electron Microscopy of Thin Crystals, Butterworths, London, p. 252 (1965).
2. A. Howie and M. J. Whelan: Proc. Roy. Soc. A. 263, 217 (1961).
3. G. N. Lance: Numerical Methods for High Speed Computers, I liffe, London (1960).
4. J. P. Hirth and J. Lothe: Theory of dislocations, McGraw-Hill, New York, p. 410, 431 (1968).
5. P. Grigoriadis and J. Stoemenos: To be published.
6. S. Amelinckx and P. Delavignette: Electron Microscopy and Strenght of Crystals, eds. G. Thomas and J. Washburn, Interscience, New York, p. 454 (1963).

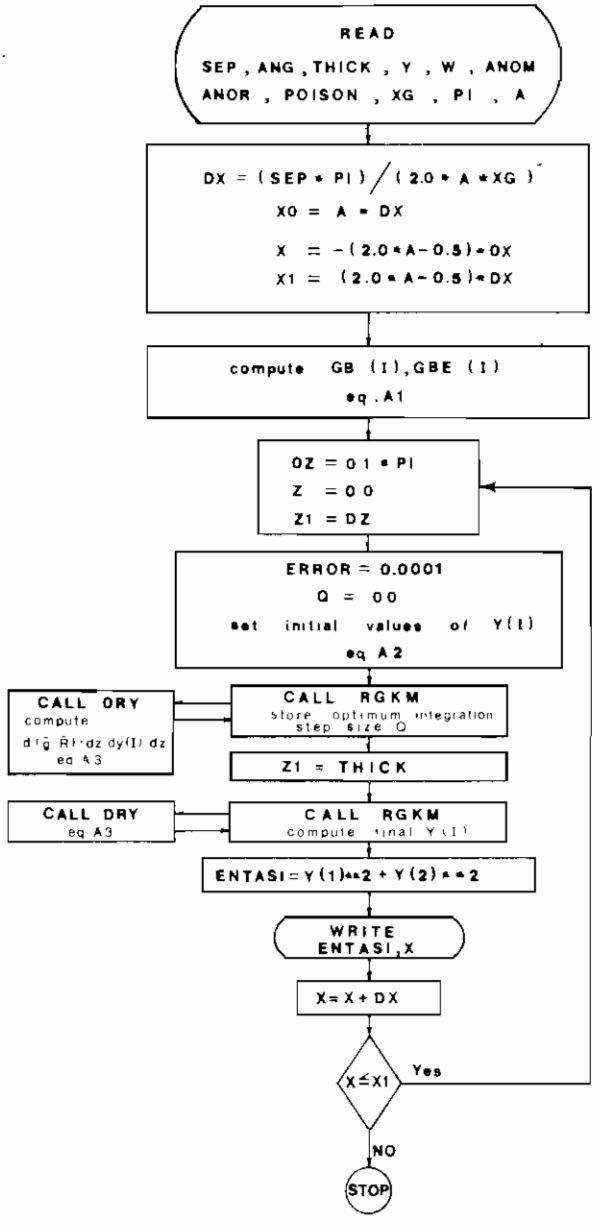

SEP = separation of partials

ANG = α

THICK = t

Y = y

W = w

ANOM = A

ANOR = N

POISON = ν

XG = ξ_g

PI = π

A = desired number of columns

Flow chart of a program to determine intensity profiles of a dislocation ribbon.

A 1

$$GB(1) = gb_1 = 1$$

$$GB(2) = gb_2 = 1$$

$$GBE(1) = \frac{gbe_1}{2(1-\nu)} = \frac{\sqrt{3}}{3(1-\nu)} \cdot \sin\alpha \, \sin\left(\alpha - \frac{\pi}{6}\right)$$

$$GBE(2) = \frac{gbe_2}{2(1-\nu)} = \frac{\sqrt{3}}{3(1-\nu)} \cdot \sin\alpha \, \sin\left(\alpha + \frac{\pi}{6}\right)$$

A 2

$$Y(1) = \mathrm{Re}\,T = 1$$

$$Y(2) = \mathrm{Im}\,T = 0$$

$$Y(3) = \mathrm{Re}\,S = 0$$

$$Y(4) = \mathrm{Im}\,S = 0$$

$$\frac{d(\bar{g}\cdot\bar{R})}{dZ} = \frac{1}{2\pi} \sum \left[\left(\bar{g}\cdot\bar{b}_1 + \frac{\bar{g}\cdot\bar{be}_1}{2(1-\nu)} \cdot \frac{x_1^2 - (z-y)^2}{x_1^2 + (z-y)^2} \right) \cdot \frac{x_1}{x_1^2 + (z-y)^2} \right]$$

where $x_1 = x - x_0$, $x_2 = x + x_0$

A 3

$$dY(1)/dZ = -A\left[Y(1) + Y(3)\right] - Y(4)$$

$$dY(2)/dZ = -A\left[Y(2) + Y(4)\right] + Y(3)$$

$$dY(3)/dZ = -A\left[Y(1) + Y(3)\right] - Y(2) - B\cdot Y(4)$$

$$dY(4)/dZ = -A\left[Y(2) + Y(4)\right] + Y(1) + B\cdot Y(3)$$

where $B = 2w + 2\pi \cdot \frac{d(\bar{g}\cdot\bar{R})}{dZ}$

Equations refered to the program flow chart.

ΠΕΡΙΛΗΨΙΣ

ΥΠΟΛΟΓΙΣΜΟΣ ΤΗΣ ΚΑΜΠΥΛΗΣ ΚΑΤΑΝΟΜΗΣ ΤΗΣ ΕΝΤΑΣΗΣ ΗΛΕΚΤΡΟΝΙΚΗΣ ΔΕΣΜΗΣ ΑΠΟ ΜΙΑ ΤΑΙΝΙΑ ΕΞΑΡΜΟΣΗΣ

Ὑπὸ

Π. ΓΡΗΓΟΡΙΑΔΗ

(Ἐργαστήριον Β' Ἕδρας Φυσικῆς, Πανεπιστημίου Θεσσαλονίκης)

Ἡ θεωρία τῆς διάθλασης τῶν ἠλεκτρονίων ἀπὸ ἕνα κρύσταλλο ποὺ περιέχει μιὰ γραμμικὴ ἐξάρμοση προβλέπει ὅτι ἡ κατανομὴ τῆς ἔντασης τῆς ἐξερχομένης ἀπὸ τὸν κρύσταλλο ἠλεκτρονικῆς δέσμης, ὅπως τυπώνεται στὴν φωτογραφικὴ πλάκα, εἶναι τέτοια ὥστε τὸ μέγιστο τῆς ἔντασης (παρατηρουμένη θέση τῆς ἐξάρμοσης) νὰ μὴ συμπίπτει μὲ τὴν γεωμετρικὴ προβολὴ τῆς ἐξάρμοσης στὴν φωτογραφικὴ πλάκα. Τὸ φαινόμενο αὐτὸ τῆς μετατόπισης ἐξαρτᾶται ἀπὸ τὰ χαρακτηριστικὰ τῆς ἐξάρμοσης καὶ στὴν περίπτωση μιᾶς ταινίας ἐξάρμοσης ποὺ εἶναι περιοχὴ μὲ σφάλμα ἐπιστοίβασης περατουμένη ἀπὸ δύο γραμμικὲς ἐξαρμόσεις μὲ διαφορετικὰ χαρακτηριστικά, ἀναμένεται, ὅτι τὸ πειραματικὰ παρατηρούμενο πλάτος τῆς ταινίας, ὅπως προκύπτει ἀπὸ τὴν ἀπόσταση τῶν εἰκόνων τῶν δύο ἐξαρμόσεων στὴν φωτογραφικὴ πλάκα, δὲν θὰ συμπίπτει μὲ τὸ πραγματικὸ πλάτος της ποὺ εἶναι ἄγνωστο. Ὁ θεωρητικὸς ὑπολογισμὸς τῆς καμπύλης κατανομῆς τῆς ἔντασης, μὲ τὶς αὐτὲς συνθῆκες περίθλασης ὅπως εἶναι πειραματικὰ μὲ κρύσταλλο $SiTe_2$, ἔδειξε ὅτι τὸ παρατηρούμενο πλάτος τῆς ταινίας εἶναι μεγαλύτερο κατὰ 1% τῆς πραγματικῆς ἀπόστασης τῶν ἐξαρμόσεων. Αὐτὸ σημαίνει ὅτι ἡ ὑπολογιζομένη ἐνέργεια τῶν σφαλμάτων ἐπιστοίβασης στὸν κρύσταλλο $SiTe_2$ πρέπει νὰ αὐξηθεῖ κατὰ 1% πρᾶγμα ποὺ βρίσκεται μέσα στὰ ὅρια τῶν σφαλμάτων μετρήσεων.